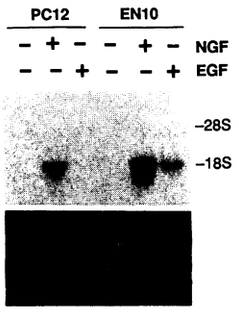

Fig. 4. Expression of transin mRNA was mediated by chimeric receptors. Cells were treated for 3 days in the presence of NGF (50 ng/ml) or EGF (5 ng/ml) in DMEM with fetal calf serum (10%) and horse serum (5%). Total RNA (20 μg) from PC12 cells and the cell line stably transfected with EN10 were isolated by guanidine thiocyanate treatment and CsCl-gradient centrifugation, separated on a formaldehyde (2.2 M)-agarose (0.8%) gel, and transferred to nitrocellulose. The filter was hybridized to a random-primed cDNA probe that encoded the rat transin gene (*16*). Ethidium bromide staining of the gel is displayed to indicate relative amounts of RNA analyzed. The markers at right indicate the sizes of ribosomal RNA.

(*19*). The common feature among these molecules is the conserved pattern of cysteine residues in the extracellular binding domains. The cytoplasmic domains, however, are unique. Deletions in the cytoplasmic domain of the $p75^{NGFR}$ result in receptors that bind ^{125}I-labeled NGF with low affinity (*20*) and lack biological responses (*21*). Affinity cross-linking and transfection studies indicate that NGF-induced biological responses require $p75^{NGFR}$ plus an associated protein (*20, 22*). The finding that the *trk* proto-oncogene binds NGF and is autophosphorylated in response to NGF (*23*) identifies $p140^{prototrk}$ as the $p75^{NGFR}$ accessory protein. The *trk* proto-onogene might be associated with the same transmembrane and cytoplasmic sequences that are found in the EN10 and EN30 chimeric receptors.

These results indicate that the low-affinity $p75^{NGFR}$ plays a crucial role in signal transduction and that the transmembrane and cytoplasmic domains are required for the initial steps of NGF-mediated neuronal differentiation. It is likely that interactions of these domains with other signal-transducing molecules are essential for NGF action. Moreover, the ability to reconstruct a growth factor response by fusion of two diverse and structurally dissimilar receptors implies that common mechanisms may function for diverse transmembrane receptor molecules in signal transduction.

REFERENCES AND NOTES

1. J. Schlessinger, *J. Cell Biol.* **103**, 2067 (1986).
2. M. V. Chao *et al.*, *Science* **232**, 518 (1986); D. Johnson *et al.*, *Cell* **47**, 545 (1986); M. Radeke *et al.*, *Nature* **325**, 593 (1987).
3. E. Livneh *et al.*, *J. Biol. Chem.* **261**, 12490 (1986). We subcloned a Xho I fragment that codes for the full-length human EGFR, digested the resulting plasmid (pNN17) with Mst II, treated the plasmid with Klenow polymerase, and digested it with Xba I to eliminate 3′ coding sequences. A 0.75-kb Mst II–Xba I fragment from a plasmid that contained the transmembrane and cytoplasmic domains of the human NGFR (*2*) was introduced into pNN17 plasmid. The resulting 2.6-kb cDNA (EN10) was excised and subcloned into the pCMV5 expression vector (*5*). EN31 was constructed from pBSEGFR, containing a 3.7-kb EGFR cDNA, by partial digestion with Nar I, treatment with Klenow enzyme, and digestion with Xba I. A 2-kb EGFR cDNA that represented the extracellular and transmembrane domains was ligated to the T5 NGFR cDNA [nucleotides 1 to 1508 (*2*) in pT3/T7] plasmid, digested with Xba I, and partially digested with Pvu II. The resulting plasmid, pEN31, was partially digested with Eco RI, and the 2.6-kb cDNA was subcloned into the pMV7 eukaryotic expression vector (*4*). EN30 was constructed by digestion of pT5 with Bst EII, treatment with Klenow, and complete digestion with Xho I. A 1.95-kb Xho I–Xho II fragment that contained the extracellular domain of the EGFR was isolated from pEN31 and introduced into the pT5 vector. The resulting cDNA was first subcloned in pNNO3 and then into pCMV5.
4. P. Kirschmeier, G. M. Housey, M. D. Johnson, A. S. Perkins, I. B. Weinstein, *DNA (New York)* **7**, 219 (1988).
5. S. Andersson, D. N. Davis, H. Dahlback, H. Jornvall, D. W. Russell, *J. Biol. Chem.* **264**, 8222 (1989).
6. M. D. Waterfield *et al.*, *J. Cell. Biochem.* **20**, 149 (1982).
7. A. S. Tischler and L. A. Greene, *Nature* **258**, 341 (1975).
8. L. A. Greene, *Brain Res.* **133**, 350 (1977).
9. H. Yan and M. V. Chao, unpublished results.
10. M. Sheng and M. E. Greenberg, *Neuron* **4**, 477 (1990).
11. K. Huff, D. End, G. Guroff, *J. Cell Biol.* **88**, 189 (1981).
12. J. Boonstra *et al.*, *ibid.* **97**, 92 (1983).
13. D. Pollock *et al.*, *Neuroscience* **10**, 2626 (1990).
14. M. E. Greenberg, L. A. Greene, E. B. Ziff, *J. Biol. Chem.* **260**, 14101 (1985).
15. D. P. Bartel, M. Sheng, L. F. Lau, M. E. Greenberg, *Genes Dev.* **3**, 304 (1989).
16. C. M. Machida, K. D. Rodland, L. Matrisian, B. E. Magun, G. Ciment, *Neuron* **2**, 1587 (1989).
17. T. H. Large *et al.*, *ibid.*, p. 1123.
18. O. Kashles *et al.*, *Proc. Natl. Acad. Sci. U.S.A.* **85**, 9567 (1988).
19. C. A. Smith *et al.*, *Science* **248**, 1019 (1990).
20. B. L. Hempstead, N. Patil, B. Thiel, M. V. Chao, *J. Biol. Chem.* **265**, 4730 (1990).
21. M. Berg and M. V. Chao, unpublished results.
22. M. Hosang and E. M. Shooter, *J. Biol. Chem.* **260**, 655 (1985); B. L. Hempstead, L. S. Schleifer, M. V. Chao, *Science* **243**, 373 (1989).
23. D. R. Kaplan, D. Martin-Zanca, L. F. Parada, *Nature* **350**, 158 (1991); D. R. Kaplan *et al.*, *Science* **252**, 554 (1991).
24. We thank B. Hempstead for comments, S. Decker for anti–NGFR receptor, and L. Matrisian and G. Ciment for transin cDNA probes. Supported by grants from the NIH, the Hirschl-Caulier Trust, Parke Davis, and the special group of donors of the Dorothy Rodbell Cohen Foundation.

15 January 1991; accepted 26 March 1991

Clusters of Coupled Neuroblasts in Embryonic Neocortex

JOSEPH J. LO TURCO AND ARNOLD R. KRIEGSTEIN

The neocortex of the brain develops from a simple germinal layer into a complex multilayer structure. To investigate cellular interactions during early neocortical development, whole-cell patch clamp recordings were made from neuroblasts in the ventricular zone of fetal rats. During early corticogenesis, neuroblasts are physiologically coupled by gap junctions into clusters of 15 to 90 cells. The coupled cells form columns within the ventricular zone and, by virtue of their membership in clusters, have low apparent membrane resistances and generate large responses to the inhibitory neurotransmitter γ-aminobutyric acid. As neuronal migration out of the ventricular zone progresses, the number of cells within the clusters decreases. These clusters allow direct cell to cell interaction at the earliest stages of corticogenesis.

THE NEOCORTEX IS ORGANIZED INTO discrete layers of neurons that are radially subdivided into functional domains or columns (*1*). The development of this highly ordered structure is an intricate process. Neurons populate their respective layers in an inside-out pattern of development (*2, 3*). Neuroblasts synthesize DNA and undergo mitotic divisions within the deepest layer of developing neocortex, the ventricular zone (*4*). After their final division, cells migrate out of the ventricular zone along radial glia (*5*). They pass older cells that have previously migrated and end their migration in the cortical plate (*6*). Each cortical cell's position and phenotype may be determined before it migrates out of the ventricular zone (*7*). The mechanisms that operate within the ventricular zone to determine the ultimate fate of immature cortical cells are not well understood.

Cell to cell interactions could participate in determining the fates of developing neurons. Investigations into interactions between ventricular zone cells have been largely precluded by the difficulty of obtaining physiological measurements from small cells maintained in situ. The application of

Department of Neurology and Neurological Sciences, Stanford University School of Medicine, Stanford, CA 94305.

whole-cell recording techniques to cells in brain slices has made it possible to study the physiology of very small cells within developing brain tissue (*8*).

When we made whole-cell recordings from cells in the ventricular zone of cortical slices (*9*) from rats at embryonic day 15 (E15), we encountered cells that had lower than the expected membrane resistances (mean ± SD; 131 ± 64 megohms, $n = 10$) (*10*). One explanation for this observation was that the cells in the ventricular zone were electrically coupled to other cells. To investigate this possibility, we injected Lucifer yellow, a low molecular weight dye, into cells in the ventricular zone. Each injection led to the staining of a large cluster of cells (Fig. 1A). Such staining only occurred when successful whole-cell attachments were made and could not be duplicated by the injection of Lucifer yellow into the extracellular space. This result established that embryonic cortical cells are coupled by a mechanism that allows small molecules to move from one cell to another within a column of cells in the ventricular zone.

Coupling between cells in the ventricular zone could be due either to cytoplasmic bridges or to gap junction channels. To distinguish between these two possibilities, we simultaneously injected both horseradish peroxidase (HRP) and Lucifer yellow into cells through the same patch electrode. HRP does not pass through gap junctions because of its large size but can pass through cytoplasmic bridges; Lucifer yellow, a much smaller molecule, passes easily through both cytoplasmic bridges and gap junction channels (*11*) (Fig. 1, B and C). Although HRP staining was restricted to only one cell, Lucifer yellow stained a large cluster of cells ($n = 6$). The connections that couple cells within a cluster, therefore, are selective for small molecules, and such selectivity is consistent with the physical properties of gap junction channel pores (*12*). The gap junction channel protein connexin 26 is expressed in the ventricular zone of embryonic neocortex in rats (*13*).

To provide additional evidence that the cell clusters were coupled by gap junction channels, we used a manipulation that decreases the conductance of gap junction channels. If gap junction channels between cells in a cluster were to conduct less current, then the apparent input resistance of cells in a cluster would increase. When the pH of the external solution was lowered from 7.4 to 6.6, a manipulation that lowers intracellular pH and decreases the conductance of gap junction channels (*14*), the apparent membrane resistance of cells within clusters increased ($n = 4$) (Fig. 2A). The same brief acidification of external solution that increased the membrane resistance of cells within clusters did not increase the membrane resistance of noncoupled neurons in the cortical plate (three out of three) (*15*). Immature cortical cells are therefore coupled by gap junction channels that can be reversibly uncoupled by lowering pH.

The number of cells in a cluster decreased as development progressed (Fig. 2B). On E15, the beginning of neurogenesis in rat cortex (*3*), every cell recorded from in the ventricular zone was part of a cluster. The clusters at E15 contained 59 ± 26 ($n = 9$) cells and extended from the ventricular surface to the cortical plate. On E16 and E17 the number of cells in clusters was reduced to 35 ± 10 ($n = 5$) and 40 ± 15 ($n = 4$), respectively. By E18 and E19, the number of cells in a cluster had decreased further (8 and 6 cells, respectively, $n = 2$), and the probability of obtaining a recording from a cell in a cluster was greatly reduced (0.07) (*16*). Most labeled cells in the ventricular zone at these later stages were isolated multipolar cells, migrating neurons, and radial glia, none of which were dye-coupled. In other words, coupled cell clusters in the ventricular zone of embryonic neocortex are transient structures that are most prominent at the beginning of neurogenesis. The decrease in the number of cells in each cluster with time suggests that, before or during their final mitosis, neurons uncouple from clusters and migrate out of the ventricular zone.

The number of cells in each cluster varied within an age group and among different ages. We took advantage of this variation to study the electrical properties of connections between clustered cells. The relation between the number of cells in a cluster and the apparent resistance of a cell within a cluster was strikingly regular (Fig. 2C). This relation was fitted with a simple model of serial and parallel resistances (*17*). The model indicated an apparent coupling resistance of 700 megohms or 1.3 nS. Because gap junction channels have unitary conductances of approximately 100 pS (*18*), it follows that approximately 13 gap junction channels connect each cell to the rest of the cluster.

Embryonic neocortex contains a heterogeneous population of precursor cells that are destined to become either neurons or glia (*19*). To determine which precursor cells were coupled into clusters, we tested for the presence of a protein that differentiates between neurons and glia. Electron microscopic studies indicate that γ-aminobutyric acid A ($GABA_A$) receptors are only present on neurons (*20*). We have similarly found, using patch-clamp techniques, that $GABA_A$ receptors are present on cortical neurons but not on glia (*21*). When 3 μM GABA was applied to cells in clusters, large currents mediated by $GABA_A$ receptors were generated (Fig. 3). Therefore, on the assumption that GABA channels are not transiently expressed on glial precursors, many, if not all, of the cells within a cluster are neuroblasts. These results do not exclude the possibility that, in addition to neuroblasts, some glial precursors are also contained in the clusters, although we have filled six radial glial cells with Lucifer Yellow and none of these were dye-coupled to cells in clusters.

The GABA currents generated by cells in clusters were large for small embryonic cells

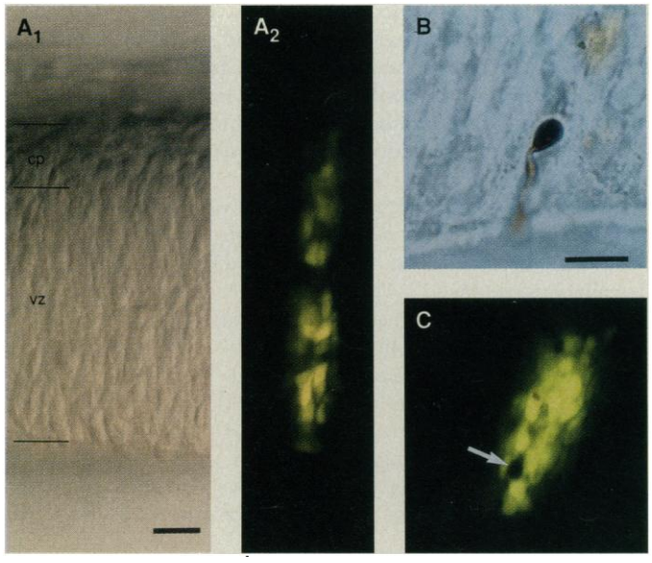

Fig. 1. Dye-coupled cell clusters in embryonic neocortex. (**A_1**) A segment of a 400-μm cortical slice from a fetal rat (E15) viewed with interference contrast optics. The pial surface is on the top, and the ventricular surface is on the bottom. cp, cortical plate; vz, ventricular zone. Scale bar, 25 μm. (**A_2**) The same segment as in (A_1) viewed with epifluorescence (Leitz, E3: peak excitation, 436 nm; barrier filter, 490 nm). (**B**) A cell in the ventricular zone that was injected with both HRP and Lucifer yellow. Transmitted illumination. Scale bar, 25 μm. (**C**) The same segment of cortex as in (B) visualized with epifluorescence. Scale bar as in (A_1). The arrow denotes the position of the cell shown in (B). The cluster is shorter than the one illustrated in (A_2) because it is in a more medial position, where the embryonic cortex is thinner.

(186 ± 12 pA); this result raised the possibility that currents were not generated by single neuroblasts but resulted from the summation of currents generated by several electrically coupled cells. To test this possibility, we compared the size of GABA currents generated by neuroblasts in clusters to GABA currents generated by cells that were not coupled. When 3 μM GABA was added to the perfusate, whole-cell currents were elicited in cells within clusters that were ten times the currents elicited in isolated cortical plate neurons (18 ± 7 pA; $n = 6$) (Fig. 3A). This difference was not attributable to a larger single-channel conductance or to a greater density of GABA channels on neuroblasts (Fig. 3B) (*22*).

Neuroblasts in the ventricular zone of embryonic neocortex are coupled by gap junction channels and as a consequence are physically and electrically linked to their neighbors. The resulting groups of cells form columns that may be analogous to the "proliferative units" observed in nissl-stained primate neocortex (*23*) or to the radially arranged groups of clonally related cells in the chick brain (*24*). Neuroblast clusters could form the basis of columnar organization in the mature neocortex, and communication between cells within a cluster could determine the layer-specific fates of cells within a cortical column. Finally, because gap junctions are critical to developmental decisions in early embryogenesis (*25*), communication through gap junction channels may be a general mechanism that operates throughout development.

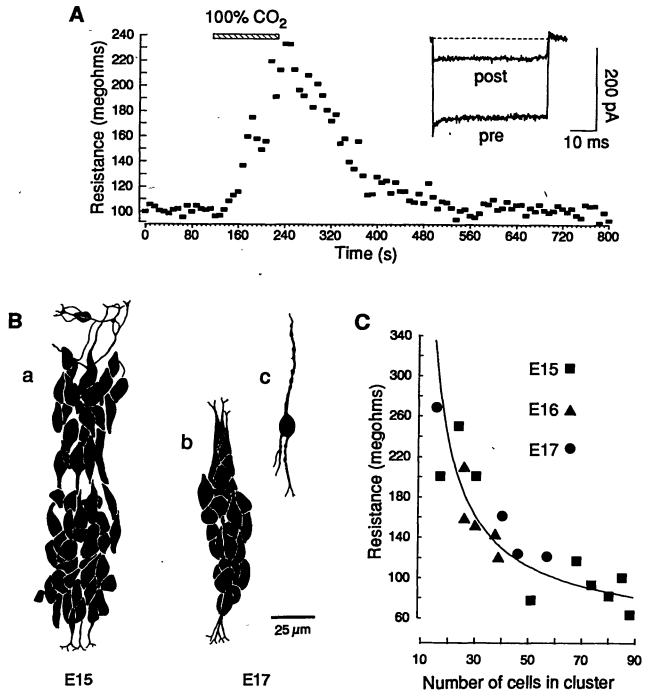

Fig. 2. Properties of neuroblast clusters. (**A**) Uncoupling of cell clusters by acidification. The solution bathing the slice was changed (hatched bar) from one saturated with 5% CO_2 (pH 7.4) to one saturated with 100% CO_2 (pH 6.6). We determined membrane resistances by measuring the current at the end of a 100-ms voltage step from −70 to −90 mV. Resistance was determined every 8 s before, during, and after the perfusate was saturated with 100% CO_2. (Inset) One current trace elicited before (upper) and another after (lower) 100% CO_2 saturation. (**B**) Camera lucida drawings of representative neuroblast clusters from E15 (a) and E17 (b) cortical slices; an isolated migrating neuron (c) from an E17 slice. (**C**) The number of cells in clusters from embryos of different ages plotted against their resistance. The data were fitted by a model assuming a cell resistance of 2600 megohms and a cell to neighbor resistance of 700 megohms (*17*).

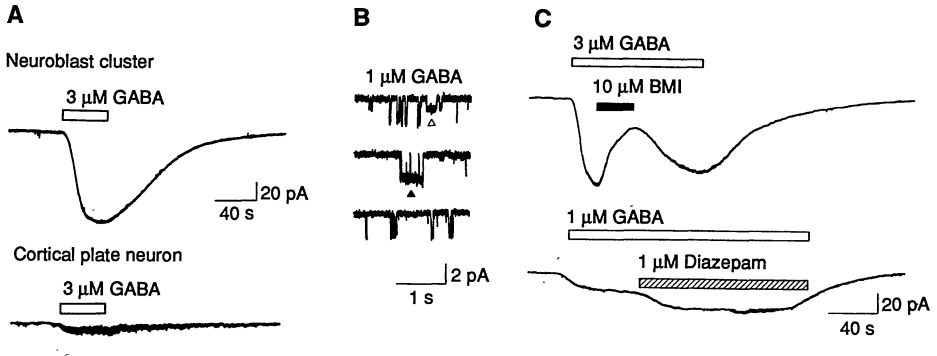

Fig. 3. Generation of currents mediated by $GABA_A$ receptors in neuroblast clusters. (**A**) Cells in clusters (upper trace) generate larger responses than noncoupled cortical plate neurons (lower trace). Both currents were elicited by bath application of 3 μM GABA, and both cells were in the same slice from a fetal rat on E16. (**B**) GABA-evoked single-channel currents in a patch of membrane excised from a neuroblast in a cluster and exposed to 1 μM GABA. The membrane potential was −70 mV, and two channel conductances were apparent: an infrequently occurring conductance of 12 pS (△) and a more frequently occurring conductance of 21 pS (▲). (**C**) The pharmacology of GABA-evoked currents in neuroblast clusters. Antagonism of the response to 3 μM GABA by the $GABA_A$ receptor antagonist bicuculline methiodide (BMI) (10 μM). (Lower trace) Potentiation of the response to 1 μM GABA by the benzodiazepine diazepam (1 μM). These pharmacological properties are characteristic of the $GABA_A$ receptors on mature cortical neurons.

REFERENCES AND NOTES

1. V. B. Mountcastle, *J. Neurophysiol.* **20**, 408 (1957); E. G. Jones, H. Burton, R. Porter, *Science* **190**, 572 (1975); D. H. Hubel and T. N. Wiesel, *Proc. R. Soc. London Ser. B* **198**, 1 (1977).
2. J. B. Angevine and R. L. Sidman, *Nature* **192**, 766 (1961); M. Berry and A. W. Rogers, *J. Anat.* **99**, 691 (1965); P. Rakic, *Science* **183**, 425 (1974); M. B. Luskin and C. J. Schatz, *J. Comp. Neurol.* **242**, 611 (1985).
3. M. W. Miller, in *Development and Maturation of Cerebral Cortex*, vol. 7 of *Cerebral Cortex*, A. Peters and E. G. Jones, Eds. (Plenum, New York, 1988), pp. 133–166.
4. R. L. Sidman, I. L. Miale, N. Feder, *Exp. Neurol.* **1**, 322 (1959); P. Rakic, in *Brain Mechanisms in Mental Retardation*, N. A. Buckwald and M. Brazier, Eds. (Academic Press, New York, 1975), pp. 3–40.
5. P. Rakic, *Brain Res.* **33**, 471 (1971); *J. Comp. Neurol.* **145**, 61 (1972).
6. A. Peters and M. Feldman, *J. Anat. Embryol.* **141**, 3 (1975).
7. K. F. Jensen and H. P. Killackey, *Proc. Natl. Acad. Sci. U.S.A.* **81**, 964 (1984); S. K. McConnell, *Science* **229**, 1268 (1985); *Brain Res. Rev.* **13**, 1 (1988); *J. Neurosci.* **8**, 945 (1988); _____, and C. E. Kaznowski, *Soc. Neurosci. Abstr.* **16**, 1272 (1990); J. A. Barfield, J. G. Parnavelas, M. B. Luskin, *ibid.*, p. 1272; J. G. Parnevalas, J. A. Barfield, M. B. Luskin, *ibid.*, p. 1272.
8. M. G. Blanton, J. J. LoTurco, A. R. Kreigstein, *J. Neurosci. Methods* **30**, 203 (1989); *Proc. Natl. Acad. Sci. U.S.A.* **87**, 8027 (1990).
9. Whole-cell recordings [O. P. Hamill, A. Marty, E. Neher, B. Sakmann, F. J. Sigworth, *Pfluegers Arch.* **391**, 85, 1981] were made as described (*8*).
10. J. J. LoTurco, M. G. Blanton, A. R. Kreigstein, *J. Neurosci.*, in press. Neurons in the cortical plate and in the ventricular zone that are not dye-coupled have membrane resistances between 800 and 3000 megohms, and radial glia in the ventricular zone have membrane resistances between 200 and 400 megohms.
11. H. Goodall and M. H. Johnson, *J. Embryol. Exp. Morphol.* **79**, 53 (1984).
12. J. D. Robertson, *J. Cell Biol.* **19**, 201 (1963); N. B. Gilula, O. R. Reeves, A. Steinbach, *Nature* **235**, 262 (1972); I. Simpson, B. Rose, W. R. Loewenstein, *Science* **195**, 294 (1977).
13. R. Dermietzel *et al.*, *Proc. Natl. Acad. Sci. U.S.A.* **86**, 10148 (1989).
14. L. Turin and A. E. Warner, *J. Physiol. (London)* **300**, 489 (1980).
15. We have not found dye-coupled neurons in the cortical plate or in more mature neocortex with whole-cell patch clamp recordings. Dye coupling between small numbers of neocortical neurons has been observed when cells were impaled with microelectrodes [M. J. Gutnick and D. A. Prince, *Science* **211**, 67 (1981); B. W. Connors, L. S. Bernardo, D. A. Prince, *J. Neurosci.* **4**, 1324 (1984)].
16. The probability was given by: (number of recordings from cells in clusters)/(number of successful whole-cell recordings from cells in the ventricular zone).
17. $$R_n = \frac{(R_c + R_g)R_{(n-1)}}{R_c + R_g + R_{(n-1)}}$$
where R_n is the resistance of a cell in a cluster with n cells and R_c and R_g are variables that describe the

resistance of a single cell to ground and the resistance between a single cell and the rest of the cluster, respectively. R_c was constrained to values between 1 and 3 gigaohms because this is the range of resistances for embryonic neurons that are not dye-coupled.
18. J. Neyton and A. Trautmann, *Nature* **317**, 331 (1985); R. D. Veenstra and R. L. DeHaan, *Science* **233**, 972 (1986).
19. M. B. Luskin, A. L. Pearlman, J. R. Sanes, *Neuron* **1**, 635 (1988).
20. P. Somogyi, H. Takagi, J. G. Richards, H. Mohler, *J. Neurosci.* **9**, 2197 (1989).
21. A. R. Kriegstein and J. J. LoTurco, *Soc. Neurosci. Abstr.* **16**, 57 (1990).
22. Single-channel currents were measured and analyzed as described (*10*). The density of GABA-activated channels may be lower on neuroblast clusters than on cortical plate neurons, because, although only 10% of membrane patches from clusters contained GABA-activated channels, 95% of patches from cortical plate cells had GABA-activated channels.
23. P. Rakic, *Postgrad. Med. J.* **54**, 25 (1978); *Science* **241**, 170 (1988).
24. G. E. Gray, J. C. Glover, J. Majors, J. R. Sanes, *Proc. Natl. Acad. Sci. U.S.A.* **85**, 7356 (1988).
25. S. Lee, N. B. Gilula, A. E. Warner, *Cell* **51**, 851 (1987); S. C. Guthrie and N. B. Gilula, *Trends Neurosci.* **12**, 12 (1989).
26. We thank H. Sullivan, C. M. O'Brien, and J. Avilla for comments on the manuscript and J. Avilla and S. Singh for technical assistance. Supported by NIH grants NS12151 and NS21223. J.J.L. was supported in part by NIH training grant NS07280.

16 November 1990; accepted 4 February 1991

Direct Molecular Identification of the Mouse Pink-Eyed Unstable Mutation by Genome Scanning

MURRAY H. BRILLIANT,* YOICHI GONDO,† EVA M. EICHER

DNA sequences associated with the mouse pink-eyed unstable mutation were identified in the absence of closely linked molecular markers and without prior knowledge of the encoded gene product. This was accomplished by "genome scanning," a technique in which high-resolution Southern blots of genomic DNAs were hybridized to a dispersed and moderately repetitive DNA sequence. In this assay, pink-eyed unstable DNA was distinguished from the DNA of wild-type and revertant mice by enhanced hybridization to one of several hundred resolved fragments. The fragment showing enhanced hybridization in pink-eyed unstable DNA was cloned and found to lie within a DNA duplication that is located close to, or within, the pink-eyed dilution locus. The duplication associated with the mouse pink-eyed unstable mutation may mediate the high reversion frequency characteristic of this mutation.

THE PINK-EYED UNSTABLE MUTATION, p^{un}, is one of at least 13 alleles of the pink-eyed dilution locus, *p* (*1*), which, together with the albino locus, *c*, constitutes the first genetic linkage group that was identified in mammals (*2*). On a C57BL/6J background, mice carrying the wild-type *p* allele have intensely pigmented coats and eyes, whereas mice homozygous for p^{un} or most other recessive *p* alleles have greatly reduced pigmentation in both their coats and eyes. Although the p^{un} mutant allele apparently affects only pigmentation, several other mutant *p* alleles are associated with additional phenotypes, including neurological problems, male sterility, and cleft palate (*1*).

The p^{un} mutant allele has the distinction of displaying the highest rate of reversion reported in mammals, reverting at a frequency at least three to five orders of magnitude greater than other *p* alleles or recessive mutations at other coat color loci (*3*). Approximately 1.8% of the offspring of homozygous C57BL/6J p^{un}/p^{un} mice have patches of wild-type color in their coats and are mosaic revertants (*4*). Occasionally, an all-black mouse is produced from a cross between a p^{un} mosaic revertant and a nonrevertant p^{un}/p^{un} mouse. These mice can be used to establish homozygous revertant lines (*5*).

The molecular basis of the high frequency of p^{un} reversion has remained an enigma until now, although several hypotheses have been advanced (*4, 6*). Only one mouse mutation with a detectable reversion frequency, *d* (dilute), has been examined in detail at the molecular level. The *d* mutation was caused by the insertion of a murine leukemia provirus in the *d* locus, and reversion from *d* to wild type is accompanied by loss of this retrovirus (7). However, because the reversion frequency of p^{un} is three orders of magnitude greater than that of *d*, the p^{un} mutation and reversion may be the result of a different process. Rates of genetic change of the same magnitude as the p^{un} reversion frequency are observed for DNA sequences repeated in tandem (*8, 9*), suggesting that the p^{un} mutation might similarly involve tandem repeats of DNA.

We have termed the method we used to identify sequence alterations associated with p^{un} DNA, "genome scanning." This method is similar to the DNA fingerprint assay (*9*) and, like DNA fingerprinting, is based on Southern hybridization (*10*) with the use of an interspersed repetitive DNA sequence as a hybridization probe. However, because our method uses a repetitive DNA probe of much higher copy number than that used in conventional DNA fingerprinting (~1000 copies per genome rather than ~60 copies per genome), a larger fraction of the genome can be scanned for sequence differences related to a mutant locus. In this type of approach, large net sequence differences (such as large duplications or deletions) have a greater chance of being detected than

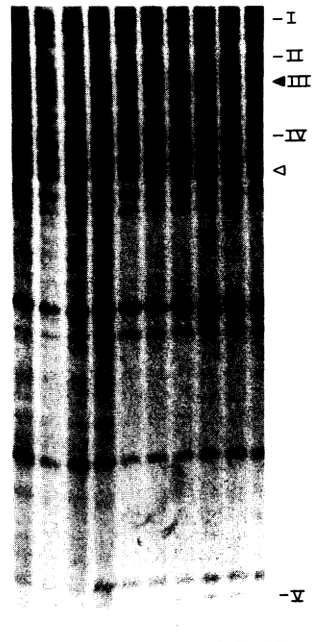

Fig. 1. Genome-scanning Southern blot of Apa I–digested DNA from individual mice homozygous for various *p* alleles hybridized to IAP DNA (*20*). An autoradiogram representing a 24-cm portion (0.88 kb to 3.4 kb) of a hybridized filter is shown (*21*). Lane 1, male revertant p^{un+1J}; lane 2, female revertant p^{un+1J}; lane 3, male revertant p^{un+2J}; lane 4, female revertant p^{un+2J}; lanes 5 and 6, female p^{un}; lanes 7 and 8, male p^{un}; lane 9, male wild type; lane 10, female wild type. Fragments enhanced in female DNA are indicated as bands I (3.3 kb), II (3.1 kb), and IV (2.6 kb). A fragment unique to male DNA is labeled V (0.9 kb). The fragment displaying enhanced hybridization in p^{un} DNA is band III (2.9 kb). Sizes of the indicated fragments were based on the migration of marker fragments, two of which are shown: closed triangle (comigrating with band III), 2.9 kb; open triangle, 2.4 kb.

M. H. Brilliant and Y. Gondo, The Institute for Cancer Research, Fox Chase Cancer Center, Philadelphia, PA 19111.
E. M. Eicher, The Jackson Laboratory, Bar Harbor, ME 04609.

*To whom correspondence should be addressed.
†Present address: Department of DNA Biology, Tokai University Medical School, Bohseidai, Isehara, Kanagawa 259-11, Japan.